A FLAT TRIANGULAR SHELL ELEMENT STIFFNESS MATRIX*

Robert J. Melosh**

Philco Western Development Laboratory

This paper presents the derivation of the equations for a flat-plate triangular element applicable to the analysis of shell-like structures using the direct stiffness method. The element accounts for membrane and bending flexibility and material properties ranging from isotropic to aeolotropic. The derived element satisfies requirements on macroscopic equilibrium and intra-element deformation compatibility for non-planar arrays, but approximates the deformation state conditioned by bending and shear stresses acting over the elements. Computed results demonstrate that the derived element is satisfactory for predicting deflections and slopes when shear rigidities are very high or low.

1.0 INTRODUCTION

The intrinsic characteristics of the flat triangular geometry make it a desirable choice for a finite element for structural analysis. It can be used without geometric error as a basic building block for representing any polygonal shape. It can be used to approximate curved surfaces. This representation can be exact in the limit (Reference 1) if refinement of mesh is properly employed, (Reference 2).

In addition, it has special attributes for structural analysis. Since the simple planar displacement function is associated with uniform stresses satisfying microscopic equilibrium, corresponding potential and complementary energy solutions are available for obtaining solution bounds as shown by DeVeubeke (Reference 3). It can also be shown that the finite element representation for the structural slice is a finite difference representation, and hence must yield the exact elasticity solution in the limit. The use of the pyramid type displacement function results in a stiffness matrix which will lead to monotonic solution in accordance with the convergence criteria of Melosh (Reference 4).

Matrices have been derived for the triangular element representing mid-plane extensions, bending and twisting. These have failed to satisfy displacement continuity requirements within the element because, as indicated by Irons, (Reference 5) this is impossible if the Kirchhoff hypothesis is retained. Moreover, these fail to retain continuity across element boundaries, except for unfolded structures. If shear deformations are considered, however, a matrix associated with a continuous displacement function within the element can be obtained. If displacements vary linearly along an edge, folded structure displacement continuity can be achieved. Such a basis was used by the author in developing a facet matrix in 1960, but was

* This paper presents the results of one phase of research carried out at the Jet Propulsion Laboratory, California Institute of Technology, under Contract No. NAS 7-100, sponsored by the National Aeronautics and Space Administration.

** Engineering Mechanics Section Manager

unpublished because of dissatisfaction with the derivation. Applications have shown that this matrix produces satisfactory results and recent work has provided the extension to the aeolotropic material.

This paper contains a formulation of this stiffness matrix for a flat triangular shell element, that is, one capable of stretching and bending. The matrix includes as a sub-set the stiffness matrix for the triangular slice in plane stress, originally published by Turner, et al (Reference 6). Applications are given for a thin, elliptical plate in bending and a thick square plate in pure shear.

2.0 DEVELOPMENT OF THE STIFFNESS MATRIX

2.1 Displacement Function

Consider the thin flat triangular facet shown in Figure 1. For convenience, a rectangular cartesian coordinate system is chosen with its origin at the centroid of the triangular area and its X-Y plane coincident with the midplane of the facet. The facet is assumed to be of uniform thickness. Assume that the displacement function is given by

$$\begin{aligned} u_i &= \lfloor 1 \; x \; y \rfloor [H] \{ v_{ji} + z\theta_{ji} \} \\ u_z &= \lfloor 1 \; x \; y \rfloor [H] \{ v_{jz} \} + f(z) \end{aligned} \tag{1}$$

where

$$i = x, y; \quad j = 1, 2, 3; \quad x_{KL} = x_K - x_L;$$

$$[H] = \frac{1}{x_{21}y_{31} - x_{31}y_{21}} \begin{bmatrix} x_2y_3 - x_3y_2 & x_3y_1 - x_1y_3 & x_1y_2 - y_1x_2 \\ y_{23} & y_{31} & y_{12} \\ x_{32} & x_{13} & x_{21} \end{bmatrix}$$

and f(z) is some undefined function of z.

It is noted that Equation 1 describes displacements that vary linearly over the planform, along any edge, and through the thickness of the facet. This is a "pyramid" function and hence will lead to monotonic convergence and an exact solution if network refinement is infinite.

2.2 Stress-Strain Relations

The stress-strain relationship is expressed by

$$\sigma = D \epsilon \tag{2}$$

where

$$\sigma = \begin{bmatrix} \sigma_{xx} \\ \sigma_{yy} \\ \sigma_{xy} \\ \sigma_{zz} \\ \sigma_{xz} \\ \sigma_{yz} \end{bmatrix} \qquad \epsilon = \begin{bmatrix} \epsilon_{xx} \\ \epsilon_{yy} \\ \epsilon_{xy} \\ \epsilon_{zz} \\ \epsilon_{xz} \\ \epsilon_{yz} \end{bmatrix}$$

For a material with one plane of symmetry (in this case the midplane of the facet) the **D** matrix takes the form,

$$\mathbf{D} = \begin{bmatrix} D_{11} & & & & & \text{Sym.} \\ D_{21} & D_{22} & & & & \\ D_{31} & D_{32} & D_{33} & & & \\ D_{41} & D_{42} & D_{43} & D_{44} & & \\ 0 & 0 & 0 & 0 & D_{55} & \\ 0 & 0 & 0 & 0 & D_{65} & D_{66} \end{bmatrix} \tag{3}$$

In order that a real material be represented, matrix **D** must be positive semidefinite.

It is customary in the analysis of shells to adopt Love's hypothesis; that is, to assume that $\sigma_{zz} = 0$. In the present context, this assumption implies a change of $f(z)$ only. Since the form of $f(z)$ is immaterial to the development, only the stress-strain relations must be modified. Imposing this condition on Equation 2 and eliminating ϵ_{zz} gives

$$\bar{\mathbf{D}} = \begin{bmatrix} D_{11} - D_{41}^2/D_{44} & & & \text{Sym.} \\ D_{21} - D_{41}D_{42}/D_{44} & D_{22} - D_{42}^2/D_{44} & & \\ D_{31} - D_{41}D_{43}/D_{44} & D_{32} - D_{42}D_{43}/D_{44} & D_{33} - D_{43}^2/D_{44} & \\ 0 & 0 & 0 & D_{55} \\ 0 & 0 & 0 & D_{65} \quad D_{66} \end{bmatrix} \tag{4}$$

2.3 Stiffness Components

To clarify subsequent discussion, the element structure will be assumed to result in two independent elastic responses. First, the direct stress response involving stretching and shearing of the elastic plane will be considered. Then, a model involving shearing only will be considered. The stiffness matrix will be composed of the sum of the stiffness associated with these responses.

The first model may be regarded as one in which the x-z and y-z shearing strains are zero or the material develops no z axis shear stress or shear strain energy as a consequence of deformation. Thus, the stress-strain relations reduce to

$$\begin{bmatrix} \sigma_{xx} \\ \sigma_{yy} \\ \sigma_{xy} \end{bmatrix} = \begin{bmatrix} D_{11} - D_{41}^2/D_{44} & & \text{Sym.} \\ D_{21} - D_{41}D_{42}/D_{44} & D_{22} - D_{42}^2/D_{44} & \\ D_{31} - D_{41}D_{43}/D_{44} & D_{32} - D_{42}D_{43}/D_{44} & D_{33} - D_{43}^2/D_{44} \end{bmatrix} \begin{bmatrix} \epsilon_{xx} \\ \epsilon_{yy} \\ \epsilon_{xy} \end{bmatrix} \tag{5}$$

and either

$$\epsilon_{xz} = \epsilon_{yz} = 0$$

or

$$D_{55} = D_{65} = D_{56} = D_{66} = 0$$

Substituting Equations 1 and 2, using the linear strain-deformation relations, the strain energy relations, and Castigliano's theorem, leads to the load-deflection relations

$$\begin{bmatrix} V_{jx} \\ \Theta_{jx} \\ V_{jy} \\ \Theta_{jy} \\ V_{jz} \end{bmatrix} = \begin{bmatrix} K_{11} & & & \text{Sym.} & \\ 0 & K_{22} & & & \\ K_{31} & 0 & K_{33} & & \\ 0 & K_{42} & 0 & K_{44} & \\ 0 & K_{52} & 0 & K_{54} & K_{55} \end{bmatrix} \begin{bmatrix} v_{jx} \\ \theta_{jx} \\ v_{jy} \\ \theta_{jy} \\ v_{jz} \end{bmatrix} \tag{6}$$

where V_{jx} and θ_{fx} are the generalized loads associated with V_{jK} and θ_{jx} and

$$\begin{aligned}
K_{11} &= \bar{D}_{11} Y^T Y + \bar{D}_{31} X^T Y + \bar{D}_{31} Y^T X + \bar{D}_{33} X^T X \\
K_{22} &= \tilde{D}_{11} Y^T Y + \tilde{D}_{31} X^T Y + \tilde{D}_{31} Y^T X + \tilde{D}_{33} X^T X \\
K_{31} &= \bar{D}_{21} X^T Y + \bar{D}_{31} Y^T Y + \bar{D}_{32} X^T X + \bar{D}_{33} Y^T X \\
K_{33} &= \bar{D}_{22} X^T X + \bar{D}_{32} X^T Y + \bar{D}_{32} Y^T X + \bar{D}_{33} Y^T Y \\
K_{42} &= \tilde{D}_{21} X^T Y + \tilde{D}_{31} Y^T Y + \tilde{D}_{32} X^T X + \tilde{D}_{33} Y^T X \\
K_{44} &= \tilde{D}_{22} X^T X + \tilde{D}_{32} X^T Y + \tilde{D}_{32} Y^T X + \tilde{D}_{33} Y^T Y \\
\bar{D}_{ij} &= t \cdot \text{AREA} \cdot (D_{ij} - D_{4i} D_{4j} / D_{44}); \quad \tilde{D}_{ij} = \frac{t^2}{12} \bar{D}_{ij} \\
X &= s \left[x_{32}, x_{13}, x_{21}, \right]; \quad Y = s \left[y_{23}, y_{31}, y_{12} \right] \\
s &= (x_{21} y_{31} - x_{31} y_{21})^{-1}; \quad x_{KL} = x_K - x_L
\end{aligned}$$

The second model involves a material or structure for which only x-z and y-z shear strains or stresses develop strain energy. Since it is desired to limit deflections to linear functions and since only two independent elastic responses are required, consideration of constant shears is sufficient. Because the angular change θ_{ji} at all the nodes is the same, an infinite number of moment coefficients can be obtained depending on how the moments are distributed to the nodes.

Because of the successful use of the shear beam with a direct stress member in predicting behavior of classical beams (Reference 7) this representation offers a reasonable device for defining uniquely the equivalent moments inducing uniform shear strain. Assume that a shear beam lies along each edge of the triangular facet, i.e., one connecting nodes 1 and 2; one connecting nodes 2 and 3; and one connecting nodes 3 and 1. Then, the partitions of the stiffness matrix associated with these members are given by

$$
\begin{aligned}
K_{22_S} &= \beta_{12} x_{21}^2 \lfloor 1,1,0 \rfloor^T \lfloor 1,1,0 \rfloor + \beta_{13} x_{31}^2 \lfloor 1,0,1 \rfloor^T \lfloor 1,0,1 \rfloor + \beta_{23} x_{32}^2 \lfloor 0,1,1 \rfloor^T \lfloor 0,1,1 \rfloor \\
K_{42_S} &= \beta_{12} x_{21} y_{21} \lfloor 1,1,0 \rfloor^T \lfloor 1,1,0 \rfloor + \beta_{13} x_{31} y_{31} \lfloor 1,0,1 \rfloor^T \lfloor 1,0,1 \rfloor + \beta_{23} x_{32} y_{32} \lfloor 0,1,1 \rfloor^T \lfloor 0,1,1 \rfloor \\
K_{44_S} &= \beta_{12} y_{21}^2 \lfloor 1,1,0 \rfloor^T \lfloor 1,1,0 \rfloor + \beta_{13} y_{31}^2 \lfloor 1,0,1 \rfloor^T \lfloor 1,0,1 \rfloor + \beta_{23} y_{32}^2 \lfloor 0,-1,+1 \rfloor^T \lfloor 0,1,1 \rfloor \\
K_{52_S} &= 2\beta_{12} x_{21} \lfloor -1,1,0 \rfloor^T \lfloor 1,1,0 \rfloor + 2\beta_{13} x_{31} \lfloor -1,0,1 \rfloor^T \lfloor 1,0,1 \rfloor + 2\beta_{23} x_{32} \lfloor 0,-1,+1 \rfloor^T \lfloor 0,1,1 \rfloor \\
K_{54_S} &= 2\beta_{12} y_{21} \lfloor -1,1,0 \rfloor^T \lfloor 1,1,0 \rfloor + 2\beta_{13} y_{31} \lfloor -1,0,1 \rfloor^T \lfloor 1,0,1 \rfloor + 2\beta_{23} y_{32} \lfloor 0,-1,-1 \rfloor^T \lfloor 0,1,1 \rfloor \\
K_{56_S} &= 4\beta_{12} \lfloor 1,-1,0 \rfloor^T \lfloor 1,-1,0 \rfloor + 4\beta_{13} \lfloor 1,0,-1 \rfloor^T \lfloor 1,0,-1 \rfloor + 4\beta_{23} \lfloor 0,1,-1 \rfloor^T \lfloor 0,1,-1 \rfloor \\
\beta_{ij} &= 6A_{ij} / 2L_{ij}
\end{aligned}
\tag{7}
$$

where A_{ij} = Area resisting shear along side ij

L_{ij} = Length of side ij

To complete the definition of the stiffness matrix, it is necessary to define the β_{ij} in terms of the facet geometry and material parameters. Since the coefficients of K_{55} are independent of moment distribution, the β_{ij} are chosen so that the K_{55} coefficients match those using Equation 1 when one angle of the facet is a right angle. This is achieved by taking

$$
\begin{aligned}
\beta_{12} &= \left| y_{23} y_{31} \rho_1 + x_{31} x_{13} \rho_2 + (x_{13} y_{23} + x_{32} y_{31}) \rho_3 \right|; \quad \rho_1 = \frac{D_{55} t}{4\,\mathrm{AREA}} \\
\beta_{13} &= \left| y_{23} y_{12} \rho_1 + x_{32} x_{21} \rho_2 + (x_{21} y_{23} + x_{32} y_{12}) \rho_3 \right|; \quad \rho_2 = \frac{D_{66} t}{4\,\mathrm{AREA}} \\
\beta_{23} &= \left| y_{12} y_{31} \rho_1 + x_{21} x_{13} \rho_2 + (x_{21} y_{31} + x_{13} y_{12}) \rho_3 \right|; \quad \rho_3 = \frac{D_{56} t}{4\,\mathrm{AREA}}
\end{aligned}
\tag{8}
$$

Equations 4, 6, 7 and 8, define the facet stiffness matrix.

3.0 APPLICATIONS

Three applications are presented here to indicate the validity of the stiffness matrix. The first application involves predictions of deflections of an aluminum plate one-inch wide, 12 inches long, and 0.1-inch thick. The plate is clamped at one end and loaded with unit loads at various stations along the span.

Figure 2 shows the gridworks examined. Analysis results are included in Table 1. These results indicate that the gridpoints at the tip deflect together, deviation of the largest angle in the triangle from 90 degrees has little effect on accuracy and predicted strain-energy is less than the theoretical. They show that the accuracy of predictions improves as the gridwork is refined.

Figure 3 shows the gridwork for a second application. This application consists of an elliptical glass plate simply supported and loaded with uniform pressure over its surface.

TABLE 1

BEAM DEFLECTION PREDICTIONS

Gridwork	Points With Unit Normal Loads	Deflections Under Loads		Beam Theory Results	Percent Error
1	3,8	.1393	.1395	.164	15.0
1	4,9	.4956	.4964	.554	10.6
1	5,10	1.2050	1.2060	1.313	8.3
2	3,8	.1217	.1217	.164	26.2
2	4,4	.5002		.554	8.0
2	5,10	1.2480	1.2480	1.313	5.2

Figure 4 shows the elliptical plate predicted deflections and slopes as compared with theoretical values determined from Galerkin's results (Reference 8). Results in Figure 4 were obtained by Clark White.* They show excellent correlation between the theoretical and numerical analysis predictions.

The accuracy of slope predictions is even better than that of displacements. The strain-energy indicated in the numerical analysis is again less than that predicted theoretically.

The third application was considered by Dr. Utku** to determine the error in predicting shear deformations. It consists of predicting the deflections of a square simply-supported plate undergoing shear deformation under a central load. Assuming that $\sigma_{xx} = \sigma_{yy} = \sigma_{zz} = \sigma_{xy} = 0.0$, the equation of shear equilibrium becomes Poisson's equation, i.e.,

$$\nabla^2 u_z = -p/Gt$$

where

u_z is the displacement normal to the plate

p is the normal pressure

G is the shear modulus

t is the plate thickness

* Clark White, Research Scientist, Manned Spacecraft Simulation, Ames Research Center, Moffett Field.

** Dr. Senol Utku, Senior Development Engineer, Applied Mechanics Section, Jet Propulsion Laboratory.

Then, the solution for the simply-supported plate can be written as a double cosine series,

$$u_z = \frac{4}{Gt\pi^2} \sum_{m=1,3,5\cdots}^{\infty} \sum_{n=1,3,5\cdots}^{\infty} \frac{\cos m\pi x/2a \cos n\pi y/2a}{(m^2+n^2)}$$

where the p integral is replaced by a single unit central load where 2a is the length of a side.

To obtain the corresponding case using the numerical analysis approach, the midplane stretching must be restrained. This can be achieved by setting $D_{11} = D_{22} = D_{12} = D_{13} = D_{23} = D_{33} = \infty$. Since setting these constants to large numbers might incur large truncation error, the V_{ji} are set to zero instead. If each element is to be in pure shear, it must also be required that θ_{ji} as well. The plate is then loaded with a single unit central load. The tangential forces implied in the theoretical analysis to satisfy microscopic equilibrium can be disregarded in the numerical analysis since they do no work.

Figure 5 shows a comparison of the theoretical and numerical analysis deflections. Excellent correspondence is obtained except directly under the load. Strain energy of the numerical analysis is less than theoretical.

Use of this stiffness matrix for analysis of parts of a hemispherical shell is contained in a report by T. E. Lang of Jet Propulsion Laboratories.

4.0 SUMMARY

A stiffness matrix has been presented for a flat, thin, triangular facet under bending, shearing, twisting, and stretching. The implied deformation state insures that the matrix will yield monotonic convergence of strain energy predictions with gridwork refinement and lower bounds on strain energy. Its successful application to pure bending and pure shearing cases indicates that it is useful in predicting structural behavior for moderately thick plates, i.e., those in which shear deformations may be important but the normal stress unimportant.

REFERENCES

1. Synge, J. L., The Hypercircle in Mathematical Physics, Cambridge University Press, Cambridge, Mass., pp. 98-117, 209-213, 1957.

2. Stong, C. L., The Amateur Scientist, Simon and Schuster, New York, pp. 409-410, 1960.

3. Fraeijs DeVeubeke, B., "Quality Between Displacement and Equilibrium Method With a View to Obtaining Upper and Lower Bounds to Static Influence Coefficients." Paper presented to Structures and Materials Panel, AGAARD, Paris, August 1962.

4. Melosh, R. J., "Bases for Derivation of Matrices for the Direct Stiffness Method," AIAA Journal, Vol. 1, No. 7, pp. 1631-1637, July 1963.

5. Irons, B. M., and Draper, K. J., "Inadequacy of Nodal Connections in a Stiffness Solution for Plate Bending," AIAA Journal, Vol. 3, No. 5, p. 61, May 1965.

6. Turner, M. J., Clough, R. W., Martin, H. C., and Topp, L. J., "Stiffness and Deflection Analysis of Complex Structures," Journal of Aeronautical Sciences, Vol. 23, No. 9, pp. 805-823, September 1956.

7. Melosh, R. J., and Merritt, R. G., "Evaluation of Spar Matrices for Stiffness Analyses," Journal Aerospace Sciences, Vol. 25, No. 9, pp. 538-543, September 1958.

8. Timoshenko, S., Theory of Plates and Shells, McGraw-Hill Book Co., New York, pp. 292-293, 1940.

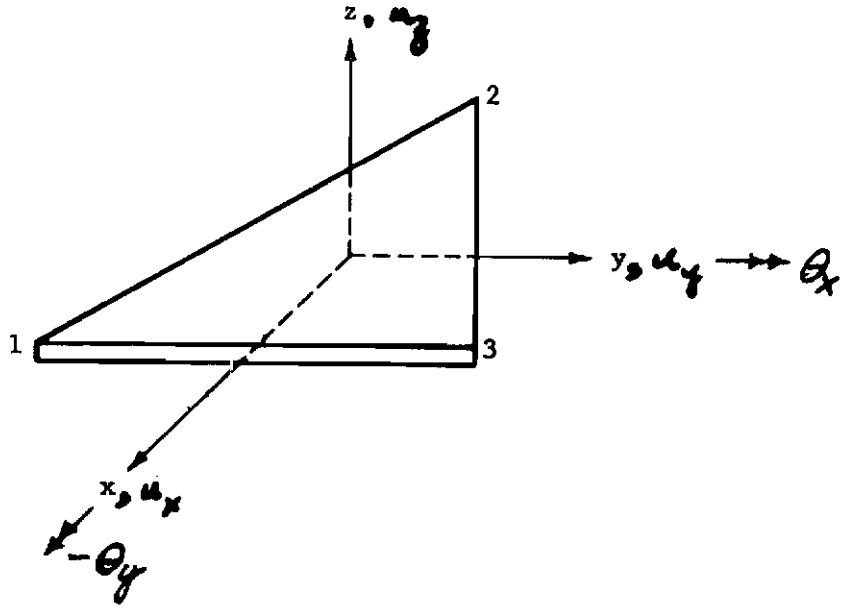

Figure 1. Facet Geometry

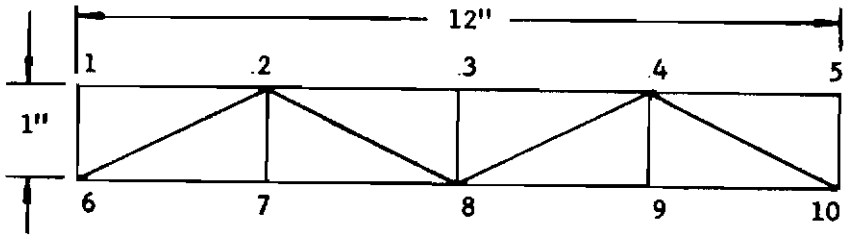

GRIDWORK 1

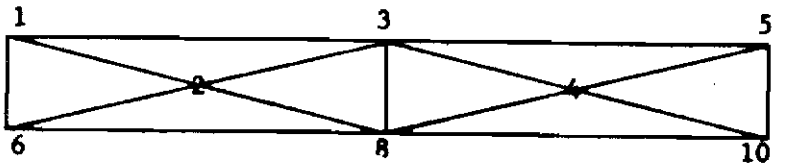

GRIDWORK 2

Figure 2. Beam Gridworks

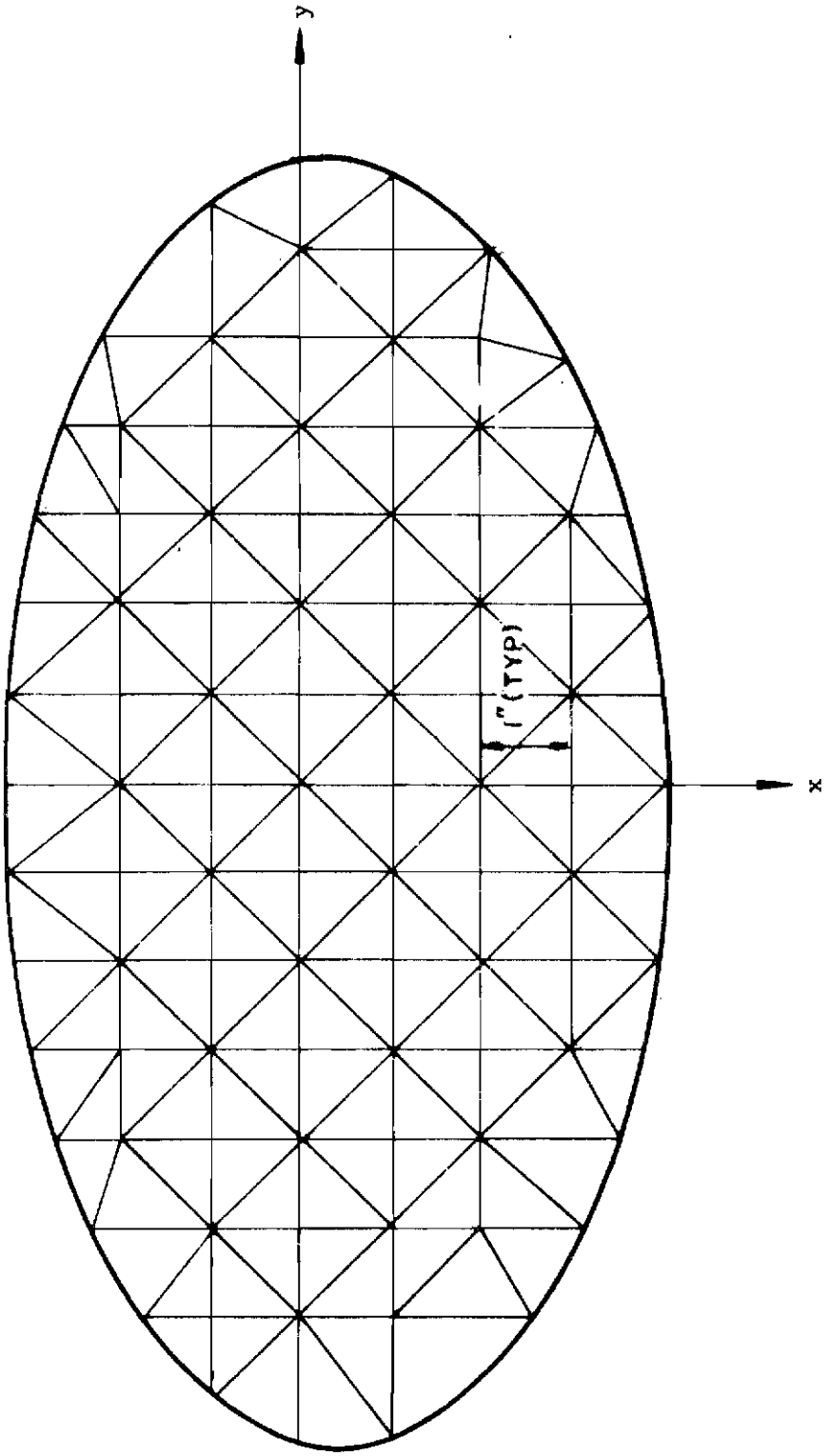

Figure 3. Ellipse Gridwork

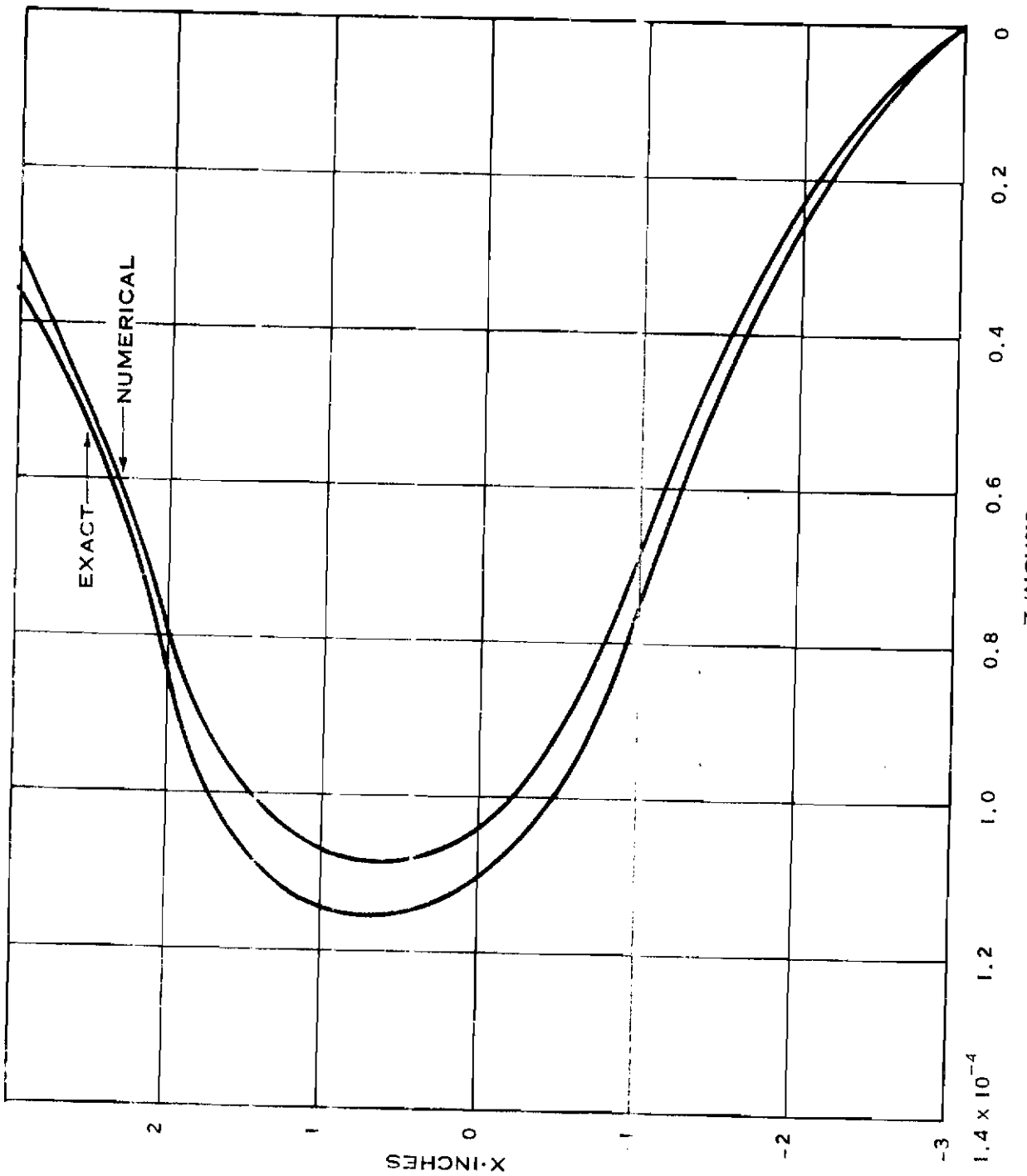

Figure 4. Ellipse Deformations

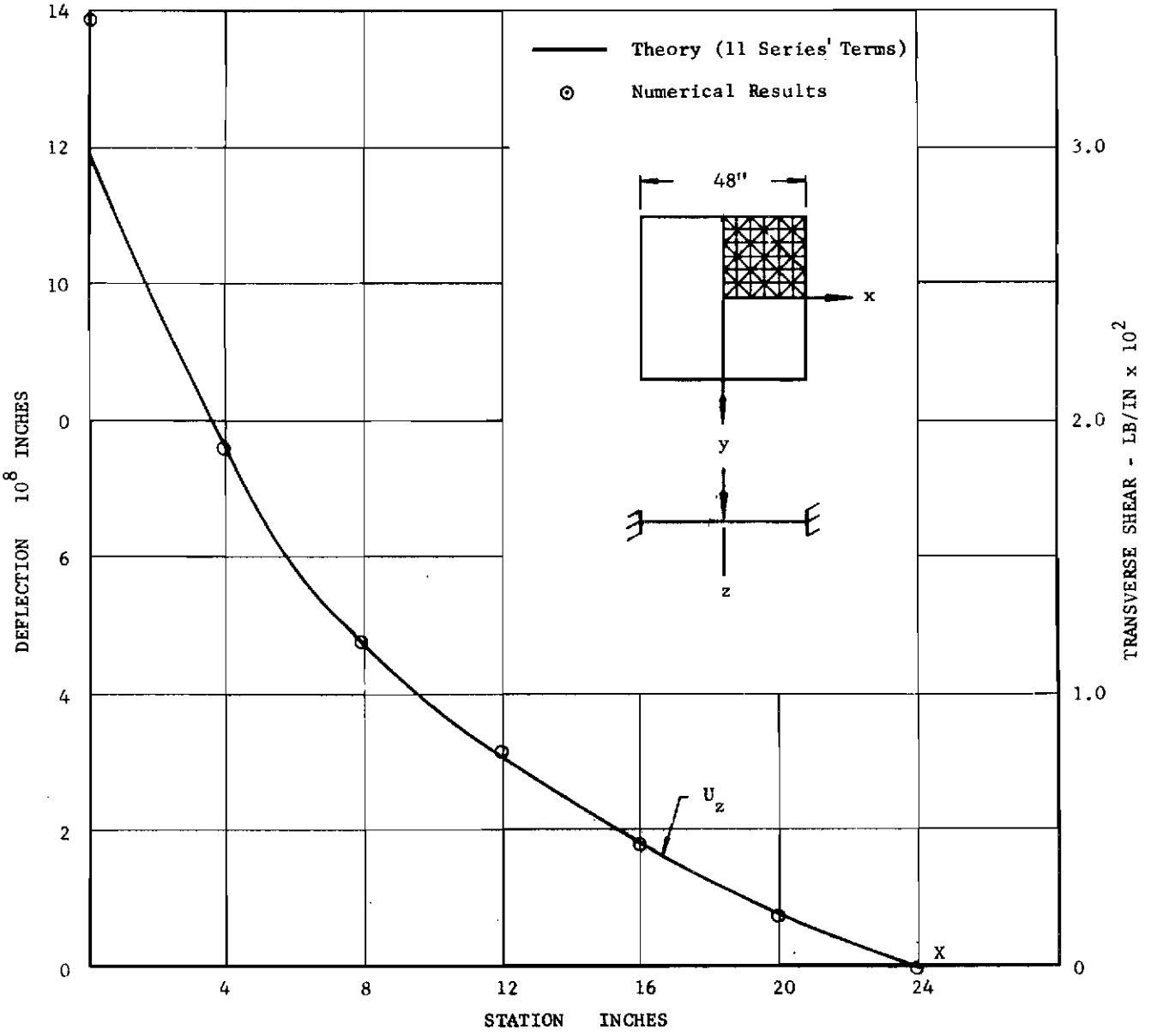

Figure 5. Square Plate Shear Deformation